Revisiting the time scale and size of the Zanclean flood of the Mediterranean (5.33 Ma) from CFD simulations

J.M. Abril*, R. Periáñez

Dpto. Física Aplicada I ETSIA, Universidad de SevillaCtra. Utrera km 1, Sevilla 41013, Spain

A B S T R A C T

The incision Zanclean Channel, which crosses the Strait of Gibraltar and the Alboran Sea, has been inter-preted as the geological fingerprint of a cataclysmic stream of water which flowed from the Atlantic into a desiccated Mediterranean about 5.33MaBP. The mathematical support for this theory is provided by a simple conceptual model for hydrodynamics and erosion that, regardless of the initial conditions, leads to scenarios of catastrophic flooding (with water flows exceeding tens or hundreds of Sv which fill 90% of the Mediter-ranean in few months or few years). This paper revisits the incision model and carries out new numerical simulations of the Zanclean flood of the Mediterranean with a two-dimensional non-linear depth-averaged hydrodynamic model. The numerical output allows solving the equation for time. This way, it is possible to estimate the final incision and the involved time scales under different modelled scenarios. When lateral erosion is reformulated in terms of the causal processes instead of a questionable scaling law, initial condi-tions become relevant. Those involving narrow connecting channels can be discarded. A flooding scenario with an excavated channel of a few hundred meter depth can be achieved with the initial conditions of a wide sill covered by a water lamina. The threshold stress to initialize erosion must be surpassed in the very early stages of the flooding, which requires a catastrophic start up. Tectonics may have played a major role in it through strike–slip faulting.

Keywords:
Mediterranean Sea
Zanclean flood
Incision model
Numerical simulation
Fluid dynamics

1. Introduction

During the Messinian Salinity Crisis (MSC, 5.97–5.33 Ma), the whole Mediterranean basin was isolated from the World Ocean, resulting in widespread salt precipitation and a decrease in the Mediterranean Sea level at kilometer scale. A comprehensive review of the MSC can be found in the paper by Roveri et al. (2014). The re-filling of the Mediterranean, known as the Zanclean flood (5.33 Ma), took place with the opening of the Strait of Gibraltar. This process is the focus of the present work. Debate about several questions is still continuing: triggering mechanism, amplitude of the sea level fall in the isolated Mediterranean, whether the reflooding happened in one or two steps, and if it was progressive, rapid or catastrophic (Cornée et al., 2016).

Several hypotheses have been considered for the triggering mechanism. The glacio-eustatic sea level rise has been discarded by some authors because the end of the MSC does not appear to coincide with any major deglaciation event (Guerra-Merchán et al., 2014; Loget and Den Driessche, 2006; Roveri et al., 2014) . Nevertheless, some works still claim the role of sea level changes in the beginning and the end of the MSC (Pérez-Asensio et al., 2013). Loget and Den Driessche (2006) also discarded the hypothesis of a tectonic origin through strike–slip faulting, because of the lack of geological evidences. Nevertheless, Balanyá et al. (2007) provided evidences of conjugated strike–slip fault systems cutting the Flysch Trough Units, being the Tarifa and the Jebel Moussa faults the major ones, at both sides of the Strait of Gibraltar. More recently, Luján et al. (2011) reported evidences of geological faults around the Tartessos Mount, in Camarinal Sill.

Since the work by Blanc (2002), based upon the examination of the morphological evolution of the Strait of Gibraltar, the most widespread accepted idea is that its opening was achieved through retrogressive erosion produced by a Messinian stream flowing from the Atlantic towards the Mediterranean. Geophysical prospection has shown that the Alboran Basin is crossed by an erosive channel, incised over the Messinian surface, known as the Zanclean Channel (García-Castellanos et al., 2009; Estrada et al., 2011). Loget et al. (2005) applied a fluvial incision model, previously calibrated with the Messinian Rhone canyons, and they concluded that the drainage system in the Gibraltar–Alboran area would have been

* Corresponding author.
E-mail address: jmabril@us.es (J. Abril).

responsible for a vertical incision ranging from 50 to 250 m during a time interval of 20–40 ky. This fluvial retrogressive erosion could have captured the Atlantic waters through an inherited topographic low in the Gibraltar area.

García-Castellanos et al. (2009) reported new evidence for the continuity of the Zanclean Channel along the Gibraltar Strait from boreholes and seismic data generated in the frame of the Africa–Europe tunnel project. Particularly, they pointed out the existence of two incision channels at both sides of the Tartessos Mount, in Camarinal Sill. Thus, instead of a fluvial incision, the likely origin of the Zanclean Channel would have been its excavation by a catastrophic flow of Atlantic waters. There are still some doubts on this interpretation. The presence of the two palaeochannels had been previously reported by Esteras et al. (2000). Despite the depth of the boreholes (540 m), they did not reach the substrate. According to these authors, this fact, along with the absence of datable lithologic or biologic elements in the older sediments, does not allow determining the age of the erosion, which could be more recent than the Zanclean flood.

For some authors (e.g., Meijer and Krijgsman, 2005), desiccation of the isolated Mediterranean was near complete in the western basin at the final stage of the MSC, while a significant water column remained in much of the eastern basin. The equilibrium level should have been between 1500 and 2700 m below present sea level according to Blanc (2006). For other authors, the sea level fall was of moderate amplitude (e.g. Manzi et al., 2005; Roveri et al., 2014) Its value can be quantitatively constrained through the study of subaerial Messinian erosional surfaces in the submarine margins. Thus, Urgeles et al. (2011) estimated a sea level drop in the Ebro Margin (western Mediterranean) of the order of 1300 m.

Concerning the reconnection to the Atlantic, Carnevale et al. (2006, 2008) provided evidences for the presence of marine fish at the final stage of the MSC (5.55–5.33 Ma), which suggests the possible persistence, continuous or episodic, of an Atlantic connection at that time. Indeed, the two pre-MSC marine gateways (the Guadalhorce and the Rifian Corridors) seem to have been closed well before the onset of the MSC. However, the amount of precipitated salts requires a significant supply of water through a narrow and shallow waterway whose location and geometry remains unknown (Roveri et al., 2014). In contrast to a geologically instantaneous sea level rise during the Zanclean flood of the Mediterranean, Bache et al. (2012) reported offshore seismic evidences from the Gulf of Lions and re-visited data from Italy and Turkey that lead to the new concept of a two-step reflooding after the MSC. They suggested a moderate initial rise in base-level, followed by a rapid sea level rise resulting from the collapse of the Gibraltar Channel.

The main features of the Zanclean Channel are its length, path, depth and cross-sections, as summarized in the work by Estrada et al. (2011). The channel is about 390 km in length, from the Camarinal Sill to at least the transition to the Algero-Balear Basin. Along the first 80 km, it displays a U shape, with an average width of 12 km, and it is deeply incised, with a depth up to 600 ms TWTT, which decreases eastwards to 250 ms. The channel splits into two branches around the ODP976 high, then it is laterally confined by the Alboran Ridge, and it splits again into three branches in the eastern domain. In this last region, the main branch is 90 km long, with U shape, and with average width and relief of 5 km and 245 ms, respectively. There is no evidence for any link to a major canyon or river valley which could have fed the channel. Estrada et al. (2011) suggested that the Zanclean Channel was incised when the sea level was about 1300–1500 m lower than it is today. These authors also reported the presence of terraces in the margins of the western Alboran Basin, between the Strait of Gibraltar and the Herradura Bank, in the Spanish margin, and between the Strait and the surroundings of Cabo Negro, in the Moroccan margin. Their origin would be likely linked to the action of the Zanclean flood.

A quantitative analysis of the whole set of erosional features of the Zanclean Channel is needed for facing some of the above mentioned open questions about the Zanclean flooding of the Mediterranean. A reference work on this topic is the model by García-Castellanos et al. (2009), which supports the catastrophic character of the Zanclean flood. It is a 0D model since it does not explicitly contain any spatial coordinates. Due to its own 0D nature, this model cannot account for any of the spatial features of the Zanclean Channel, so it places its focus on the accumulated incision at Gibraltar Sill. The model assumes crude approaches for both the hydrodynamics and the erosion processes. Regardless of the initial conditions, it leads to scenarios of catastrophic flood with water flows exceeding tens or hundreds of Sv which fill 90% of the Mediterranean in few months or few years time. The model estimates the velocity from the Manning's formula for permanent flow in open channels with an oversimplified estimation of hydraulic gradients, which gives a major controlling roll to the Sicily Sill depth. The estimation of shear stresses is another capital point since they are the causal magnitude for the incision process. Periáñez and Abril (2015) presented a more refined description of the hydrodynamics by numerical simulations using a two-dimensional non-linear depth-averaged hydrodynamic model with a flood/drying algorithm. This model can account for the spatial distribution of water currents and shear stresses, but it shared the algorithms and results from the erosion model by García-Castellanos et al. (2009).

Vertical incision can be the result of different processes, among which abrasion and cavitation may dominate. They are poorly understood from a quantitative point of view, and the empirical laws involve parameters which span over orders of magnitude. Thus, the present work adopts a formulation based upon an energetic balance, relating the energy required to erode the unit volume of rock with the dissipated power per unit area (Lamb et al., 2008) and an erosion yield. This constrains the parameter values in the power law for the vertical incision rate. On the other hand, it is known that erosion starts when a threshold shear stress is exceeded (Lavé and Avouac, 2001; Lague, 2013). This requirement is absent in the above models, but a moderate stream of water with null or very low eroding capacity, which flows during several centuries, can significantly contribute to fill the Mediterranean under non-catastrophic conditions.

The 0D model describes lateral erosion through a scaling relationship between channel width (W) and water flow (Q): $W = k_w Q^{a_w}$ (García-Castellanos et al., 2009). This relationship, referred as the scaling law hereafter, arises from a statistical correlation in alluvial rivers under steady-state conditions and where Q is related with (and limited by) the catchment area (Lague, 2013). Its application to mountain rivers under non steady-state conditions has resulted to be inappropriate (Finnegan et al., 2005; Whittaker et al., 2007) , and its use in the scenario of the Zanclean flood is more than questionable. As it will be shown further in this paper, the use of the scaling law with the geometry of the Gibraltar Strait implies a lateral erosion up to two orders of magnitude higher than the vertical one, which can be far from the physical reality.

The combination of the vertical incision law and the estimation of the shear stress in the 0D model leads to analytical solutions for the incision depth versus time with a vertical asymptote, as shown later in this paper. The catastrophic character of the Zanclean flood lies around this asymptote. Thus, it is a capital question to identify and to accurately quantify the physical limitations which prevent the system to reach a physically meaningless infinite value for the incision depth.

Interpretation of the geophysical findings does not seem to be unambiguous and thus, more refined modelling approaches are necessary to better illuminate the origin of the Strait of Gibraltar and the details of the Zanclean flood. This is the aim of the present

study, which revisits the incision model and carries out numerical simulations of the Zanclean flood of the Mediterranean with a two-dimensional non-linear depth-averaged hydrodynamic model previously developed by Periáñez and Abril (2015) and further refined here. It overcomes many of the previous simplifications and it is able to account for the main spatial features of the Zanclean Channel. The 2D model requires a plausible reconstruction of the topography of the former Gibraltar Isthmus. The continuity of geological structures along the Alboran Arc in Southern Iberia and North Africa, and particularly the Flysch Trough Units (Crespo-Blanc and Campos, 2001; (Luján et al., 2011)), makes the Tarifa-Algeciras segment the most likely place for the geological barrier. We explore several configurations generated by simple algorithms, as presented in Section 2. Results and discussion are presented in Section 3. The numerical outputs allow estimating the final incision and the involved time scales under different modelled scenarios, and they will serve for revisiting some of the still open questions around the Zanclean flood of the Mediterranean. Conclusions are summarized in Section 4.

2. Methods

The mathematical formulation of the 0D model and its results can be found in García-Castellanos et al. (2009). Some refinements (e.g. including the Bernoulli effect and head losses) and sensitivity tests were presented in the work by Periáñez and Abril (2015). The basic technical aspects relevant for the present work, along with the analytical asymptotic solution, are presented in Appendix A. The 2D model is based upon the basic physical principles of conservation of mass and momentum. The involved numerical techniques and the applications for studying the propagation in the sea of tides and tsunamis are well established and they are of a widespread use (e.g., Kowalik and Murty, 1993). The application of this model to the scenario of the Zanclean flood of the Mediterranean has been previously presented in Periáñez and Abril (2015). The most relevant technical aspects are summarized in Appendix B. The reconstruction of the Gibraltar Sill, the adopted incision model, as well as the overall working strategy are described in this section.

2.1. 2D topography of Gibraltar Strait

The 2D model domain (Fig. 1) extends from 6.000° W to 0.808° W, and from 35.000° N to 37.608° N, with an spatial resolution of 30 arcsec. The computational grid has been obtained from the GEBCO08 database, available on-line. Present day bathymetry has been adopted as a practical approach, but the morphology of the Alboran Sea is not too much different from that of the final MSC (Estrada et al., 2011; Roveri et al., 2014) .

A plausible reconstruction of the Gibraltar Sill has been implemented. Present day bathymetry of each grid cell with coordinates (i,j), $h(i,j)$, has been modified to simulate the former sill at the eastern part of the Strait of Gibraltar, with depth $h_{sill}(i,j)$, through the following algorithm:

$$h_{sill}(i,j) = h(i,j)\left[k_S + b(i-i_S)^2\right]; \quad i \in [i_S, i_L] \tag{1}$$

$$b = \frac{1-k_S}{(i_L-i_S)^2}; \quad k_S \le 1. \tag{2}$$

This correction applies to grid cells located between the longitude of the present day minimum cross-section, S_0, (i_S, corresponding to 5.56° W) to its eastern reach at longitude 5.39° W (grid coordinate i_L), with coordinate j running from south to north to cover all the present day width of the Gibraltar Strait. This way, S_0 is diminished by a factor k_S, while the applied correction reduces towards the east following a quadratic law until i_L (for which the correction factor is always equal to unity). With this algorithm, west of S_0 there is a sharp change in the seabed surface. This configuration will be labelled hereafter as "AS ". With the same algorithm, which involves a quadratic law, index i can be extended to the western cells to generate a sill with a smooth shape at both sides of S_0. The resulting configuration of the sill will be labelled as "SS". Fig. 1 shows a 3D view of a SS sill for $k_S = 0.01$.

2.2. Incision model

Incision into rock occurs relatively slowly and during large infrequent events (Lague, 2013). Important mechanisms for river bed erosion are abrasion by suspended sediments, cavitation and plucking of jointed rock (Lamb et al., 2008). The kinetic energy per unit bedrock volume required to cause abrasive erosion, ϵ_v, is a function of the tensile yield strength, σ_T, and the Young's modulus of elasticity of the bedrock, Y (Lamb et al., 2015):

$$\epsilon_v = k_v \frac{\sigma_T^2}{Y}, \tag{3}$$

with $k_v \sim 10^6$.

The concept of ϵ_v can be extended to account for the average energy per unit volume required for erosion through all the involved processes. The energy per unit time and unit area dissipated by friction in the water stream is $\vec{\tau}_b \cdot \vec{v}$. Regardless of the involved mechanisms, a fraction of this power (given by the yield factor f_y) feeds the bed erosion. If dz_s/dt is the rate of vertical incision, then the energy applied to erosion per unit time and unit area is $\epsilon_v dz_s/dt$. Thus,

$$\epsilon_v \frac{dz_s}{dt} = f_y \vec{\tau}_b \cdot \vec{v}. \tag{4}$$

If the shear stress is given by a quadratic law as Eq. (16) (Appendix B), $\vec{\tau}_b \cdot \vec{v} = \tau_b^{3/2}/\sqrt{\rho k_f}$ (k_f is the bed friction coefficient, and ρ the density of seawater), and then the incision law of the 0D model (Eq. (10) in Appendix A) is reencountered with $a = 3/2$ and

$$k_b = \frac{f_y}{\epsilon_v \sqrt{\rho k_f}}. \tag{5}$$

The erosion yield, f_y, is zero for shear stresses under a certain threshold value τ_b^*. Increasing sediment loads in the water stream increases f_y up to a maximum value (of the order of 1% –5 %), and then it decreases for higher loads due to a shielding effect (values inferred from the total erosion model applied to the South Fork Eel River, California, with $\epsilon_v = 10^9$ J m^{-3}; (Lamb et al., 2008). The value of τ_b^* is a function of the particle size, the bed roughness and the flow regime. Values in the range of 20–40 Pa have been reported for bedrock rivers (Lavé and Avouac, 2001; Lamb et al., 2008). Annandale (1995) defined an erodibility index that is correlated with the critical rate of energy dissipation. This last takes values of 0.2–0.3 kW/m^2 in the Taan River, as reported by Liao et al. (2014).

Lateral erosion is an open question in mountain rivers. Wobus et al. (2006) described it in terms of the same causal magnitude involved in the vertical incision: the shear stress. They found that the scaling law for W naturally arises when adopting a radial-logarithmic distribution of water velocities around the upper-central axis of the channel. Water velocities may not fit such a distribution under high turbulent regimes, and lateral erosion may involve other causal processes as slope destabilization (Konsoer et al., 2016). As a practical approach, Liao et al. (2014) neglected lateral erosion in their 2D-modelling study of the Taan River, Taiwan, where vertical incision rates reached up to 2 m/year after the uplift induced by Chi-Chi

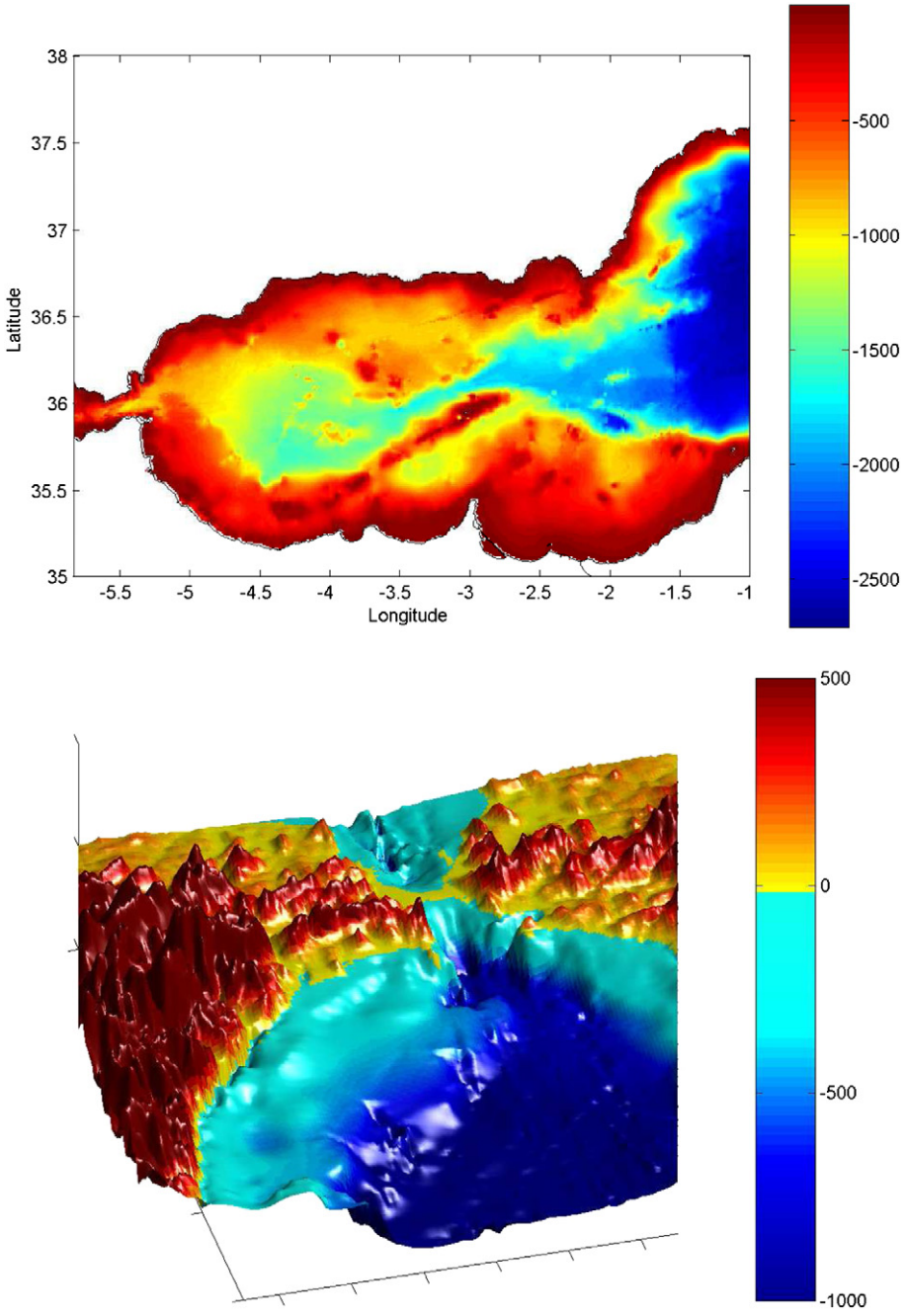

Fig. 1. Top: Computational domain for the 2D simulations. Bottom: 3D view (from S-SE) of the reconstructed Gibraltar Sill with the smoothed geometry SS and $k_S = 0.01$. Present day depths (from GEGCO08 database) are used for the the rest of the domain. Scale color-bar in m, measured positive above the present sea level.

earthquake (1999). Finnegan and Dietrich (2011) used the simple approach of estimating lateral erosion in the meander bends of the Smith River as a function of the vertical incision through a multiplicative factor. Bank materials from meandering rivers may contain sand and clay fractions which contribute to a lower erosion threshold, and to a higher erodibility and potential failure (Konsoer et al., 2016) when compared with bedrock rivers.

In this work, to explore the effect of alternative formulations for the lateral erosion, the simple approach by Finnegan and Dietrich (2011) will be adopted by imposing

$$\frac{dW}{dt} = f_L \frac{dz_s}{dt}, \tag{6}$$

being f_L a constant with values in the range of 1–5. Another methodology for the treatment of lateral erosion will consist of imposing the sequential excavation stages of Gibraltar Sill arising from the increasing values of k_S (in Eq. (1)) in the 2D model.

Eq. (5) allows a physical interpretation of k_b coefficient and may be used to constrain its value. Thus, the use of a constant and uniform value for the whole domain is a crude approach due to the variability in bedrock properties and the suspended sediment loads. The bed friction coefficient, k_f can be constrained by the reference values for the Manning's coefficient and by its controlling role in the sear stress (see Appendix B). Despite the wide range of variability in ϵ_v and f_y, their ratio can be constrained by a global energetic balance for the Zanclean Channel, as shown below.

The involved potential gravitational energy for the Zanclean flood, E_P, can be estimated from the initial gap between the Atlantic and Mediterranean water levels, z_{max}, and the hypsometric curves from Meijer and Krijgsman (2005), which provide the free surface area $A(z)$ for any gap z:

$$E_P = \rho g \int_0^{z_{max}} zA(z)dz. \quad (7)$$

It results in 3.6×10^{22} J (9.2×10^6 Mt) when adopting as initial conditions a sea level of 2500 m below the Atlantic level. This value reduces to 2.5×10^6 Mt for a gap of 1500 m.

From data reported by Estrada et al. (2011), the length of the Zanclean Channel is ~390 km and its mean cross-section is of the order of ~2 km^2. If its entire volume was excavated by the Zanclean flood, with the known value for the dissipated energy (Eq. (7)), then it is possible to estimate the average ratio $f_y/\epsilon_v \sim 2 \times 10^{-11}$ m^3 J^{-1} (for a gap of 2500 m). Here, f_y is an effective yield, to which lateral erosion contributes. A pre-Zanclean fluvial erosion that partly excavates the channel implies a lower ratio f_y/ϵ_v (and thus, a lower k_b value). A lower initial gap between the Atlantic and Mediterranean sea levels would imply a higher value for this ratio. A non-uniform spatial distribution of this ratio allows higher or lower values of k_b in the former Gibraltar Sill.

2.3. Working strategy

Section 3.1 is devoted to a series of numerical experiments with the model 0D. The goal is to test the model output when the scaling law for the channel width is replaced by a causal law for lateral erosion. This will point out the relevant role of the initial conditions, discarding those involving narrow streams of water.

A 2D–3D model approach is necessary for understanding the spatial features of the incision Zanclean Channel. Although equations for hydrodynamics and erosion can be combined in the 2D model, their complete numerical solution over the time scales involved in the Zanclean flood are beyond our present computational capabilities. Thus, a sequential modelling strategy is necessary, and the subsequent steps in the Results and discussion 3 section are devoted to build up such a modelling scenario, and to further constrain the initial conditions and the values of the involved parameters.

Section 3.2 solves the quasi-steady-state water flows and bottom shear stresses for sequential stages of excavation of the sill at Gibraltar. Alternative initial morphologies for the isthmus and different values for the friction coefficient are considered. The flow attenuation at the final stages of the filling of the Mediterranean is also studied. These results, when coupled with the erosion model, will be used to solve the equation for time and to explore scenarios for a possible erosive origin of the Strait of Gibraltar (Section 3.3).

The scaling parameter in the incision law, k_b, will be constrained in order of magnitude by a global energy balance. As erosion activates when the threshold shear stress is exceeded, initial conditions will require a minimum value for the water depth. Several numerical scenarios will be defined by adopting an initial morphology for the sill, initial water levels at the Mediterranean, and fixed values for the friction coefficient, k_f, and for k_b. By handling the outputs from the 2D model it will be possible to estimate the time of filling, the final incision depth and the maximum flow. This will further constrain the acceptable scenarios for a catastrophic flooding of the Mediterranean. These estimates assume that incision at the sill approximately progresses as described by increasing values of k_S (Eq. (1)). Self consistency will be provided by additional modelling exercises and the end of Section 3.3.

A more comprehensive view of the formation of the incision channel at Gibraltar and the western Alboran Sea will be provided with a modelling work involving 2D hydrodynamics coupled with vertical incision and lateral erosion. The model will use a flexible numerical mesh and a *time-jump* technique (Section 3.4). This modelling study uses the best scenario for catastrophic flooding identified in Section 3.3.

Finally, the different scenarios involved in the still open questions around the Zanclean flood of the Mediterranean will be discussed in the light of the present numerical simulations (Section 3.5).

3. Results and discussion

3.1. 0D model

Table 1 summarizes a set of numerical experiments carried out with the 0D model. In all cases, we used the hypsometric curve corresponding to present day bathymetry (from Meijer and Krijgsman, 2005). A first run, R1 is devoted to reproduce results from the reference model by García-Castellanos et al. (2009), excluding corrections by Bernoulli effect and head loss, and accounting for a 9 m drop in the Atlantic Sea level occurring during the flooding of the Mediterranean.

Run R1 uses initial conditions which represent a weak stream of water ($z_{s,0} = 1.0$ m; $W_0 = 3.0$ m — depth and width of the sill, respectively). The channel width has been set to fulfill the scaling law. The initial value of $\tau_b \sim 100$ Pa (Eq. (9) in Appendix A) can be considered over the threshold value for activating erosion. Time series of hydrodynamic magnitudes have been previously published (García-Castellanos et al., 2009; Periáñez and Abril, 2015) ; thus, only the main features are discussed here. The Mediterranean is completely filled after 15.2 y, with the final 90% of its volume having been completed in 434 days. This time compares well with the one obtained from the asymptotic solution shown in Appendix A. The maximum values for flow and stress are 177 Sv and 14.0 kPa, respectively. The final excavated channel is 245 m deep and 15.97

Table 1
Results from the 0D model. Incision depth, z_s, channel width, W, filling time, t_f, time for entering the last 90% of the inflow, t_{90}, velocity at the sill, v_s, water flow, Q, bottom shear stress, τ_b and Froude number, F_r. MDL is the effective channel length. [a](1) $W = 1.2Q^{0.5}$ with irreversibility; (2) corrections by Bernoulli effect and head loss; (3) flow limitation ($Q < 80$ Sv); (4) lateral erosion $dW/dz = f_L dz_s/dt$.

Model setup[a]	Run	Initial		Final				Maximum values				MDL
		$z_{s,0}$ (m)	W_0 (m)	z_s (m)	W (m)	t_f(y)	t_{90} (y)	v_s (m/s)	Q (Sv)	$\tau_b(\times 10^{13})$ Pa	Fr	(km)
(1)	1	1	3	245	15,970	15.201	1.189	54.5	177	14.0	1.46	162
(1)	2	1	5000	240	15,300	15.454	1.456	49.4	162	12.3	1.42	163
(1) + (2)	3	1	3	303	12,430	25.346	1.759	52.2	107	13.5	1.44	162
(1) + (2)	4	1	5000	300	12,180	25.847	2.396	43.6	103	10.2	1.38	163
(1) + (2) + (3)	5	1	3	319	10,733	25.441	1.853	52.2	80	13.5	1.44	150
(1) + (2) + (3)	6	1	5000	313	10,730	25.925	2.474	49.5	80	10.2	1.38	153
(1) + (2) + (3) + (4); $f_L = 5$	7	1	3	1660	8280	25.715	1.469	157	80	56.6	1.71	22
(1) + (2) + (3) + (4); $f_L = 5$	8	1	5000	349	6730	26.456	3.042	46.3	68	9.8	1.36	161
(1) + (2) + (3) + (4); $f_L = 1$	9	1	3	19,000	19,000	26.036	1.466	647	80	455	2.0	0.14
(1) + (2) + (3) + (4); $f_L = 1$	10	1	5000	391	5380	26.624	3.163	50.0	65	10.3	1.38	159

km wide. It is possible to integrate the energy dissipated by friction per unit of channel length, $E_L = \int \tau_b(W + 2z_s)dt$, and to compare it with E_P (Eq. (7)) to estimate an effective channel length ($MDL = E_P/E_L$ in Table 1). This last figure will be used only for identifying clearly unrealistic results. The maximum velocity in R1 is 54.5 m/s, which is higher than the speed of gravity waves, as a Froude number higher than unit ($F_r = v_s/\sqrt{gR_h}$) indicates. This points out that equations have been applied beyond the scope of their validity. But as this only happens around the peak value of v_s, one can accept that the main features of the catastrophic flood described by run R1 are preserved.

Run R2 is as R1 but with an initial channel width of $W_0 = 5$ km. It may represent a relatively flat isthmus covered by a water lamina after a tectonic lowering. The scaling law for W only applies if it widens the channel. Thus, the code preserves W_0 until the water flow is able to generate a larger value for W. The resulting scenario for the catastrophic flooding is very similar to that of R1 (Table 1).

After R1 and R2, one can conclude that if the hypotheses behind the 0D model properly apply, the initial conditions for reaching a quite similar scenario of catastrophic flooding of the Mediterranean do not matter.

Runs R3 and R4 repeat the previous simulations but with the corrections by Bernoulli effect and the head loss. These reduce the maximum values for Q and v_s and increase the required time to fill up the Mediterranean, but the main features of a catastrophic filling, despite of the initial conditions, are still preserved. Supercritical flow conditions are also achieved around the maximum value of v_s.

Periáñez and Abril (2015) have shown from 2D hydrodynamics modelling that the shallow Camarinal Sill limits the water flow around 80–90 Sv when its cross-sectional area is exceeded by the one excavated at Gibraltar. Runs R5 and R6, on the basis of R3 and R4, introduce such limitation. This only slightly increases the time of fill up and thus, it preserves the main results from the previous runs.

Runs R7 and R8 are build up on the basis of R5 and R6, respectively, but using an alternative formulation for the lateral erosion with $f_L = 5$ (Section 2.2). In scenario R7, with an initial narrow and shallow water channel ($z_{s,0} = 1.0$ m; $W_0 = 3.0$ m), the final incision depth is unacceptably high (1.66 km); the maximum value for τ_b is very high (56.6 kPa), and the MDL value seems unrealistic. When the initial conditions reflect those of a relatively flat isthmus covered by a water lamina, the final channel geometry is compatible with observations, and the main features of a catastrophic flood are again encountered. Runs R9 and R10 used $f_L = 1$, and they reinforce the previous results from R7 and R8.

These results show how the treatment of the lateral erosion discriminate a subset of initial conditions that are admissible. Those representing a shallow wide sill can lead to a catastrophic flooding scenario.

3.2. 2D high resolution model for the Strait of Gibraltar and the Alboran Sea

The algorithm used for reconstructing the former sill (Eq. (1)) allows for initial conditions of a shallow and wide sill surpassed by a water lamina. For each imposed value of k_S, the 2D model runs for a simulation time of one day. A quasi steady-state for water flow through the sill is reached after a few hours. It is worth noting that although erosion can be implemented into calculations, the changes in water depths are negligible for these time scales. The initial Mediterranean Sea level is set as −2000 m, being deep enough to avoid any limitation effect in the water flow at Gibraltar. With these settings, a series of numerical experiments have been carried out, as detailed below.

Experiment 2D-E1 uses the reference value for the friction coefficient ($k_f = 0.0025$, see Appendix B) and the spatial resolution of 30 arcsec with the AS configuration of the sill. The quasi steady-state flow is computed for a discrete set of k_S values ranging from 0.006 up to 0.7 (excavated cross-sections ranging from 0.04 km^2 up to 4.6 km^2). Results are shown in Fig. 2, where water flow is plotted vs. the value of the limiting cross-section at the sill. It can be seen that as the incision progresses (i.e., Q increases) and becomes greater than the cross-section at the Camarinal Sill ($S_C = 3.7$ km^2), this last acts as the main limiting factor for the water flow, which stabilizes around 80 Sv.

Experiment 2D-E2 is as 2D-E1 but it uses a coarser spatial resolution of 60 arcsec. Results appear in Fig. 2 and they are in good agrement with the previous ones, although with a stable final value of Q around 90 Sv. This experiment supports the confidence of results produced with the higher spatial resolution of 30 arcsec, which will be used in the remaining experiments.

Experiment 2D-E3 is as 2D-E1 but with an increased value of the friction coefficient, $k_f = 0.010$, which corresponds to the highest range for the Manning coefficient for bedrock rivers (see Appendix B). Indeed, the Zanclean stream of water could have been

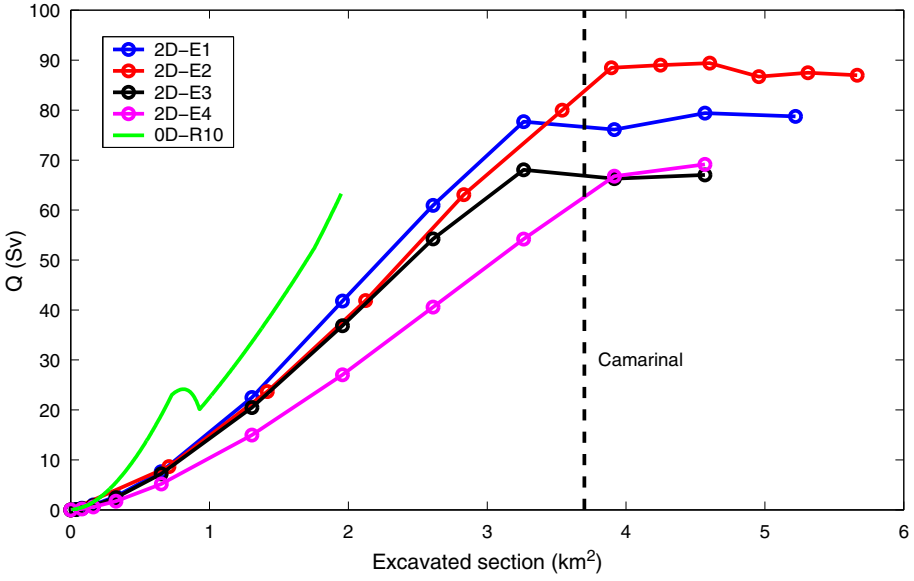

Fig. 2. Computed quasi steady-state water flows for the numerical experiments E1 to E4 and 0D-R10 (see text and Tables 1 and 2 for experiment definitions).

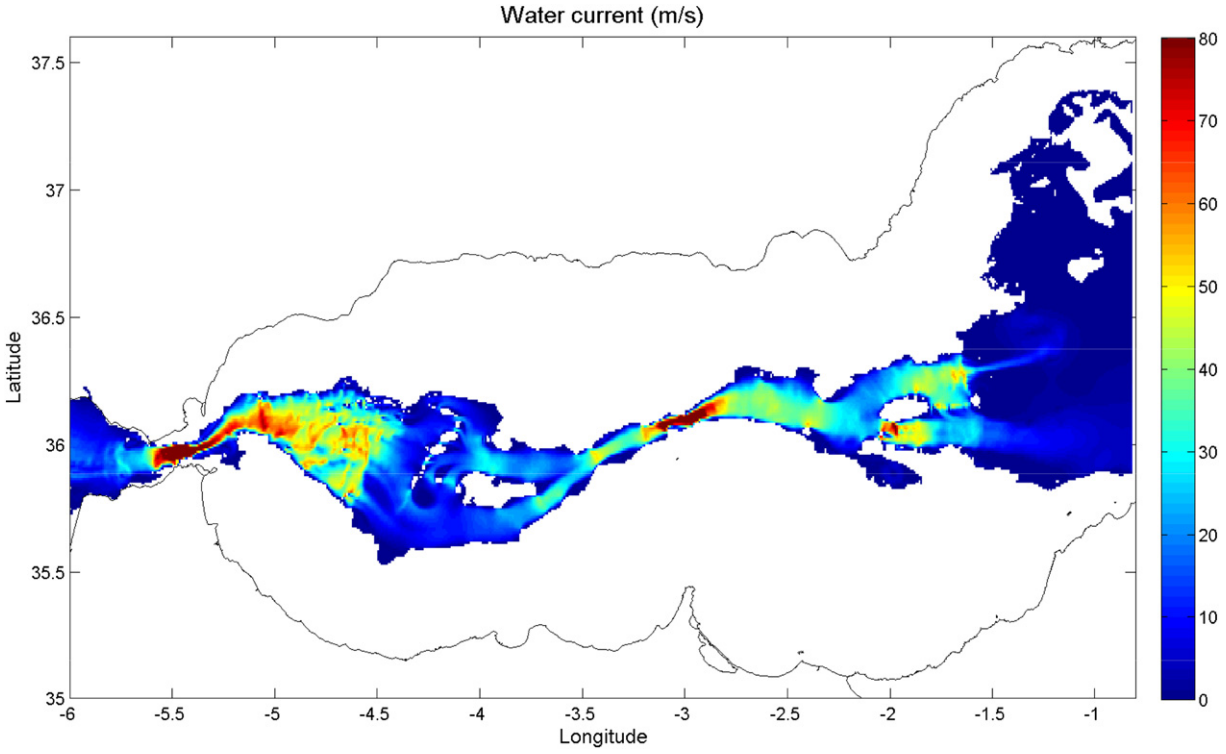

Fig. 3. Computed spatial distributions of water current magnitude (m/s) for numerical experiment 2D-E4 with $k_S = 0.4$.

an abrasive flow carrying a noticeable sediment load, which justifies exploring the effect of higher values for the friction coefficient. The values of Q result slightly lower than those computed in 2D-E1 experiment (Fig. 2), with an upper limit around 70 Sv.

Experiment 2D-E4 is as 2D-E3 but using the smoothed configuration for the sill (SS). This geometry produces a higher hydraulic resistance and significantly lower values of Q, although with the same upper limit (Fig. 2). In all experiments, the computed value for the Froude number at the central sill position remains below 1 (subcritical flow). For the sake of comparison, results from the 0D model R10 (see Table 1) are also depicted in Fig. 2.

For each model run the spatial distribution of water elevations and velocities have been generated for the quasi steady-state flow. Fig. 3 shows the computed water current magnitude for 2D-E4 with $k_S = 0.4$. The path of the water flow through the desiccated Alboran Sea is in good agrement with the reported path of the Zanclean Channel (Estrada et al., 2011). This only shows the ability of the model for finding out the connected topographic lows.

Fig. 4 shows how the water flow attenuates in the final stage of the flood, when the gap between the Atlantic and the Mediterranean water levels decreases to zero. This is illustrated for two cases, with experiment 2D-E4 with $k_S = 0.4$ and experiment 2D-E1 with $k_S =$

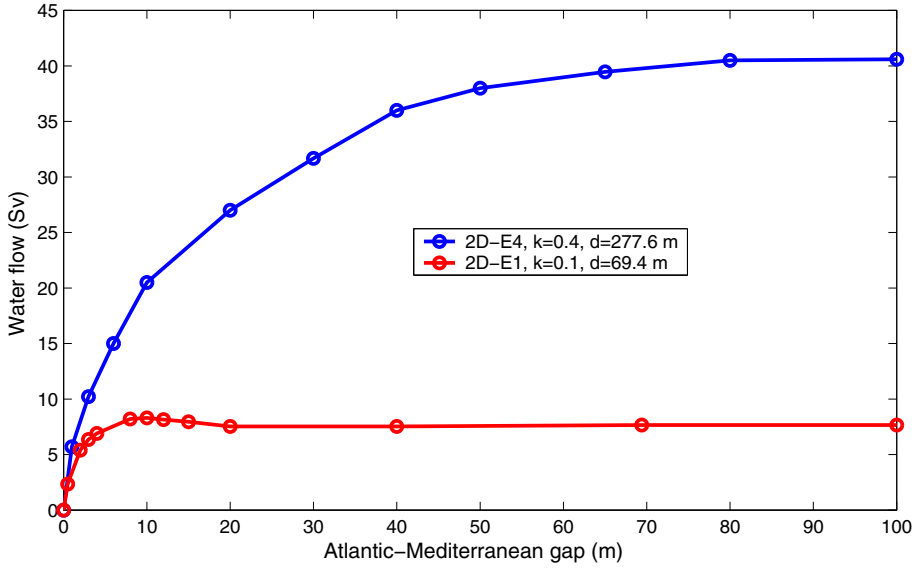

Fig. 4. Computed quasi steady-state water flows as a function of the gap between the Atlantic and Mediterranean Sea levels for the numerical experiments (E1, $k_S = 0.1$), and (E4, $k_S = 0.4$). In the legend box, d indicates the maximum depth of the sill.

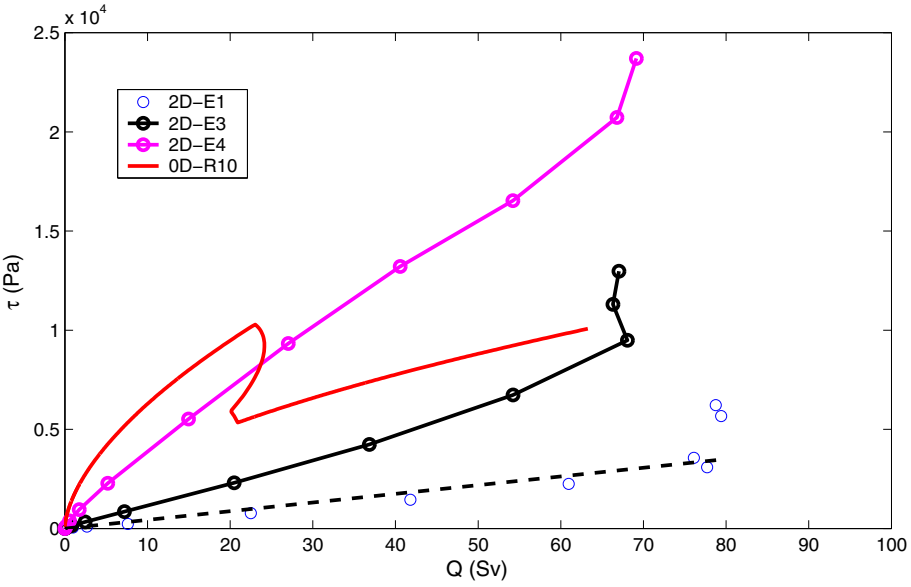

Fig. 5. Computed shear stress at the central point of the Gibraltar Sill, as a function of the water flow for the numerical experiments 2D-E1, 2D-E3, 2D-E4 and averaged value over the cross-sectional wet perimeter for 0D-R10 (see text for experiment description).

0.1. Only when the Mediterranean water level exceeds half of the sill depth, the attenuation in water flow starts to be noticeable. The reason is the rise of the water level in the sill, which increases the wet cross-section and compensates the decrease in water current. When using the Atlantic–Mediterranean gap scaled with the sill depth, $z_N = (z_1 - z_0)/z_s$, the normalized (to its stable value at larger gaps) water flow, Q_N, fits well to a saturation-type exponential function: $Q_N = 1 - exp(-\alpha z_N)$ (α is a constant that takes values of 15 and 40 for 2D-E4 and 2D-E1 experiments, respectively). This attenuation process is substantially different to the one assumed in the 0D model. The most relevant result is that for final incision depths smaller than 500–600 m, the transgression of the Sicily Sill does not affect the flow at Gibraltar.

The computed values for the shear stress strongly depend on the friction coefficient and the shape of the sill (AS versus SS configurations), as shown in Fig. 5. The 0D model R10, which also represents initial conditions of a wide shallow sill, estimates higher values in the region of relatively low water flows, which enhances erosion at the initial stages. It is worth noting that stresses in the 0D model represent averaged values over the cross-sectional wet perimeter, while the 2D model reports local values at the deepest point of the cross-section. These last are 2–2.8 times higher than their corresponding averaged values estimated from 2D hydrodynamics. Also, the complex behavior of stress in the 0D model is due to the assumed estimate for the hydraulic slope and the effect of the transgression of the Sicily Sill.

Results summarized in Figs. 2, 4 and 5, when combined with an incision law, allow to estimate the time lapses between two consecutive excavation stages of the sill, along with the cumulative water inflow, as shown in the next subsection.

3.3. Numerical scenarios for an erosive origin of the Strait of Gibraltar

The value of the water level in the Mediterranean at the end of the MSC is controversial (Roveri et al., 2014). The scenario defined for the 0D model will serve for the present purpose, and the effect of a higher initial water level will be also explored. The curves τ vs. Q (Fig. 5) and Q vs. z_s (complementary information to Fig. 2, not shown) have been digitalized by using a piecewise 4-points based polynomial fit. Given initial conditions for z_s, the deepest point in the sill cross-section, the values of $Q(z_s)$ and $\tau(Q)$ are found. This last serves to estimate the incision rate (Eq. (10)) and to update the value of z_s to repeat the processes with time steps that are adapted to the magnitude of the incision rate. The cumulative inflow serves to update the sea level at the western Mediterranean, z_1, by using the hypsometric curves. The attenuation in Q is introduced following the exponential fit to curves in Fig. 4 when $(z_1 - z_0) < z_s/2$. The depth of the Sicily Sill is

Table 2
Results from 2D numerical experiment for an erosive origin of the Strait of Gibraltar. $z_{s,0}$ and $z_{s,f}$ are initial and final values of the sill depth (at its deepest central point). Initial values are set to get an initial shear stress over the adopted threshold value of 25 Pa. z_1 is the initial sea level of western Mediterranean, measured positive below its present day value. The initial level in eastern Mediterranean is 2700 m and 2000 m for $z_1 = 2500$ m and $z_1 = 1500$ m, respectively. t_f is the time to complete fill up, and t_{90} the time lapse for completing the final 90% of the inflow. Q_{max} and τ_{max} are the peak values for the water flow through the Gibraltar Strait and the shear stress at the central point of the sill, respectively. k_b is the multiplicative parameter in the incision law, and $k_{b,0} = 1.3 \times 10^{-4}$ m y^{-1} Pa$^{-1.5}$ is the reference value. S_G is the final value of the limiting cross-section at the Gibraltar Sill; and F_r is the maximum Froude number at that location.

Experiment	$z_{s,0}$ (m)	z_1 (m)	$z_{s,f}$ (m)	k_b	t_f (y)	t_{90} (y)	Q_{max} (Sv)	$\tau_{max} \times 10^3$ (Pa)	S_G (km^2)	F_r
2 D-E1-1	9.0	2500	15.9	$k_{b,0}$	259.1	202.6	0.86	0.04	0.16	0.60
2 D-E1-2	9.0	2500	83.8	$10k_{b,0}$	70.1	37.3	10.3	0.34	0.83	0.60
2 D-E1-3	9.0	1500	58.0	$10k_{b,0}$	65.3	47.2	5.7	0.18	0.57	0.57
2 D-E3-1	6.6	2500	44.2	$k_{b,0}$	193.4	103.9	3.5	0.45	0.44	0.53
2 D-E3-2	6.6	2500	534	$4k_{b,0}$	55.5	13.3	67.0	21.7	5.3	0.48
2 D-E3-3	6.6	2500	4150	$10k_{b,0}$	26.5	6.0	67.0	21.8	41*	0.48
2 D-E4-1	3.5	2500	529	$k_{b,0}$	149.4	10.7	69.0	22.9	5.2	0.30
2 D-E4-2	3.5	1500	320	$k_{b,0}$	148.7	32.6	44.1	13.9	3.2	0.38

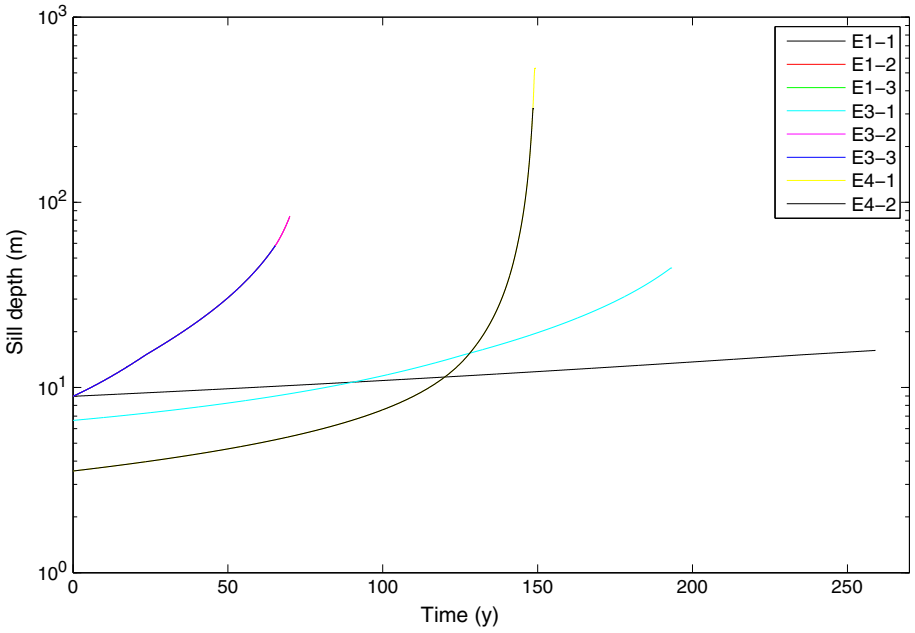

Fig. 6. Computed time series for the incision depth at the deepest point of the sill cross-section from the numerical experiments defined in Table 2.

maintained as in the 0D model. Initial values for z_s have been fixed to get an initial shear stress over the adopted threshold value of 25 Pa. Results are summarized in Table 2 and in Fig. 6.

For the numerical experiment 2D-E1-1, with $k_f = 0.0025$, the reference value of $k_{b,0} = 4.1 \times 10^{-12}$ m s^{-1} Pa$^{-3/2}$, the one used by García-Castellanos et al. (2009), leads to $f_y/\epsilon_v = 0.7 \times 10^{-11}$ m^3 J^{-1}. This last ratio compares well with the one estimated from the global energy balance (Section 2.2). Initial conditions with a sill depth at its central point of 9.0 m are needed for a value of $\tau = 25$ Pa. The initial value for Q is 0.34 Sv. The fill up of the Mediterranean is completed after $t_f = 259$ y, with the final 90% of the inflow lasting $t_{90} = 202.6$ y. The maximum value of Q is 0.86 Sv, and the final incision depth at the sill is only of 12.6 m. When the incision rate is increased by a factor of 10 (experiment 2D-E1-2), the fill up is completed after 70 y ($t_{90} = 37.3$ y), with a final sill depth of 83.8 m and a maximum Q of 10.3 Sv. But the ratio f_y/ϵ_v exceeds the value given by the energy balance. Finally, if the initial Mediterranean level was about 1 km higher (experiment 2D-E1-3) the complete filling takes place in a slightly shorter time with a less developed incision (Table 2, Fig. 6). The hypothesis of the formation of the Strait of Gibraltar some hundred meters deep due to the erosion produced by the Zanclean flood is not supported by this set of numerical scenarios from experiment 2D-E1.

For the numerical experiment 2D-E3-1, $k_f = 0.010$, the reference value of $k_{b,0}$ leads to $f_y/\epsilon_v = 1.3 \times 10^{-11}$ m^3 J^{-1}, close to the value given by the energetic balance. An initial sill depth $z_s = 6.6$ m is required to get a shear stress of 25 Pa. The initial value for Q is 0.12 Sv. The Mediterranean volume is completed after 193.4 y ($t_{90} = 103.9$ y), with a final incision depth of only 44.2 m, and a maximum flow of 3.5 Sv. When the incision rate is increased by a factor 4 (experiment 2D-E3-2), the fill up is completed after 55.5 y ($t_{90} = 13.3$ y), with a final sill depth of 534 m and a maximum Q of 67 Sv. A higher value of $k_b = 10k_{b,0}$ (experiment 2D-E3-3) leads to unacceptable values for the final incision depth (over 4 km). With the numerical scenario of experiment 2D-E3 (enhanced friction), an erosional origin of the Strait of Gibraltar is possible with an incision rate ~4 fold the reference value. This locally surpasses the value given by the energetic balance, but it could be justified by the spatial variability in f_y and ϵ_v. It is worth noting that initial conditions require a catastrophic start-up allowing to a water lamina 6.6 m thick to surpass the isthmus. Otherwise, a slow achievement of such initial conditions would have significantly contributed to fill the Mediterranean and to reduce the chance for a catastrophic scenario.

Experiment 2D-E4-1 requires a shallower sill ($z_s = 3.5$ m) as initial conditions. With the reference value for $k_{b,0}$ (again $f_y/\epsilon_v = 1.3 \times 10^{-11}$ m^3 J^{-1}), an acceptable scenario of catastrophic flooding is encountered, with a final incision depth of 529 m and $t_{90} = 10.7$ y (Table 2 and Fig. 6). A higher initial water level in the Mediterranean (experiment 2D-E4-2) diminishes the final incision depth and increases t_{90} up to 32.6 y. Again, a catastrophic start up is required for reaching initial conditions. Refinements and further discussion around this modelling exercise will be presented in Section 3.5.

Previous calculations assume that the time evolution of the cross-section shape at Gibraltar Sill does not differ too much from that defined by the increasing values of k_S (Eq. (1)). This can be supported by an additional modelling exercise. As the output of 2D model provides the value of the shear stress for all the grid-cells along the sill cross-section, it is possible to apply the incision law to compute the evolution of the entire cross-section from any given initial state. Results for the numerical scenario 2D-E4-1 are shown in Fig. 7. The averaged value of the shear stress over the wet perimeter in the sill, τ_m, has been computed from the outputs of the 2-D hydrodynamic model. The curves τ_m vs. Q (not shown) and Q vs. the excavated cross-sectional area (Fig. 2) have been digitalized by using a piecewise 4-points based polynomial fit. Thus, given initial depths along the cross-section, d_j, the values of the cross-sectional area, Q and τ_m can be then estimated. The ratio of the shear stress at any grid cell, τ_j, with respect to τ_m is assumed to be constant for the simulation period. Then, from τ_j the incision rate at each cell can be obtained, which allows estimating the new values for depths d_j after a certain time step (this last is adapted along calculations). All the process is repeated to reach the next fixed reference stage of excavation. The new computed sections (M_i in Fig. 7) can be compared with the reference ones given by Eq. (1) (S_i in Fig. 7). These last are also used as initial conditions for each sequential modelling exercise shown in Fig. 7 for the numerical experiment 2D-E4-1. Results are in reasonable agreement, and the resulting elapsed times are also consistent with the simulations above (Fig. 6). The shear stress at the channel

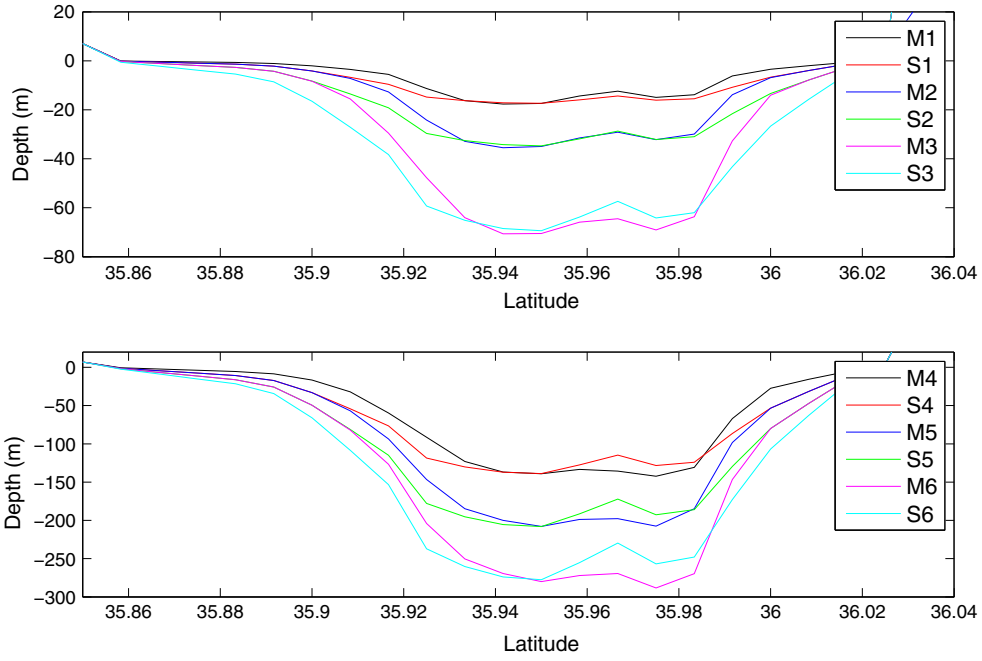

Fig. 7. Computed cross-sections (M_i) for the numerical experiment 2D-E4-1 versus the reference ones (S_i) generated by Eq. 1 ($i = 1,2,3,4,5,6$ corresponds to $k_S = 0.025, 0.05, 0.1, 0.2, 0.3, 0.4$, respectively). For generating each M_i, S_{i-1} has been set as initial condition (S_0 corresponds to $k_S = 0.0125$).

banks is one order of magnitude lower than the one at the deepest central point of the cross-section. Thus, estimates of lateral erosion from the shear stress, with $f_L = 4$, plays a minor role in these simulations. As at each sequential run the initial cross-section is reset to that generated by the reference k_S value, this implies that other complementary mechanisms for lateral tuning are involved.

Previous calculations have focussed in the evolution of the incision and the cross section at the Gibraltar Sill. A more comprehensive view of the formation of the Zanclean Channel along the Strait of Gibraltar and the western Alboran Sea can be achieved through a full 2D hydrodynamics model with a coupled erosion module, as shown in the next subsection.

3.4. 2D model with flexible mesh for vertical incision and lateral erosion

A final set of calculations has been carried out to investigate the filling process simultaneously including vertical and lateral erosion, limited by the constrains found in previous sections. Particularly, the scenario 2D-E4 has been selected. The 2D domain in Fig. 1 has been used with the SS geometry of the sill, presented in the same figure. The bed friction coefficient is $k_f = 0.010$ and lateral erosion has been scaled as $f_L = 5$ times the vertical one. This last applies at any edge of grid-cells with different depths. The initial water layer thickness over the sill in Gibraltar is 8.7 m. Thus some years, which have been skipped, are required to reach this state (108 y from the initial conditions stated in 2D-E4-1 simulations, Fig. 6). Initial water level in the Mediterranean is set to 2400 m below the Atlantic level. This is a conservative estimate that favors the time of opportunity for incision, and it is justified by uncertainties involved in the initial conditions, affecting both the water level in the Mediterranean and the depth and shape of the sill.

A sequential chain of simulations has been carried out to proceed forward in time. The initial conditions mentioned above have been used in the first simulation, until a quasi steady-state is reached in the western domain. From the computed bed stresses over the domain, both vertical and lateral erosion which would result after a few months to few years (*temporal jump*) of such inflow conditions are calculated (Mediterranean level would not change enough over this temporal jump to affect inflow). The treatment of vertical erosion only requires to appropriately change the bathymetry. The new Mediterranean level is calculated from the entered volume of water and the known hypsometry for the global Mediterranean, which is introduced in the eastern open boundary. Finally, taking into account the dominant E–W direction of the flow, the hydrodynamic equations in Appendix B have been modified to work on a domain with variable grid cell size in the south–north direction (Δy). Thus, if a given cell erodes a neighboring (and shallower) one, their sizes are appropriately changed. Care is taken to prevent that the size of any cell in the domain approaches to zero. If this happens, then the temporal jump is reduced. Once the eastern boundary condition and the domain have been updated, a new simulation is carried out and the process is repeated.

Forty simulations have been required to advance 49 years in time and to complete the filling of the Mediterranean ($t_{90} = 34$ y). The resulting topography is presented in Fig. 8, which may be compared with the initial configuration in Fig. 1. Maximum water flow is about 15 Sv and 532 m have been excavated in the center of the sill in Gibraltar Strait. The final cross section in Gibraltar Sill is 1.82 km^2. These values are of the order, but lower, than the corresponding ones estimated with the 2D-E4-1 modelling exercise. Differences arise by the absence of other mechanisms for lateral erosion than that induced by shear stresses. This way the excavated channel evolves with similar incision depths but with a smaller width.

It is worth noting that the simulation time is one day in each single run, which ensures the quasi steady-state flux at Gibraltar Sill, but it is not long enough to provide accurate estimates of erosion in the most eastern reaches of the Zanclean Channel. Thus, the morphology of the channel in this region is poorly described. Consequently this is not the best possible simulation but it has the value of first providing a global view of the main spatial features of the Zanclean Channel. A significant erosion is produced in the eastern side of Gibraltar Strait, where a deep and narrow channel extending in the western Alboran Sea has been excavated. Maximum incision depths along

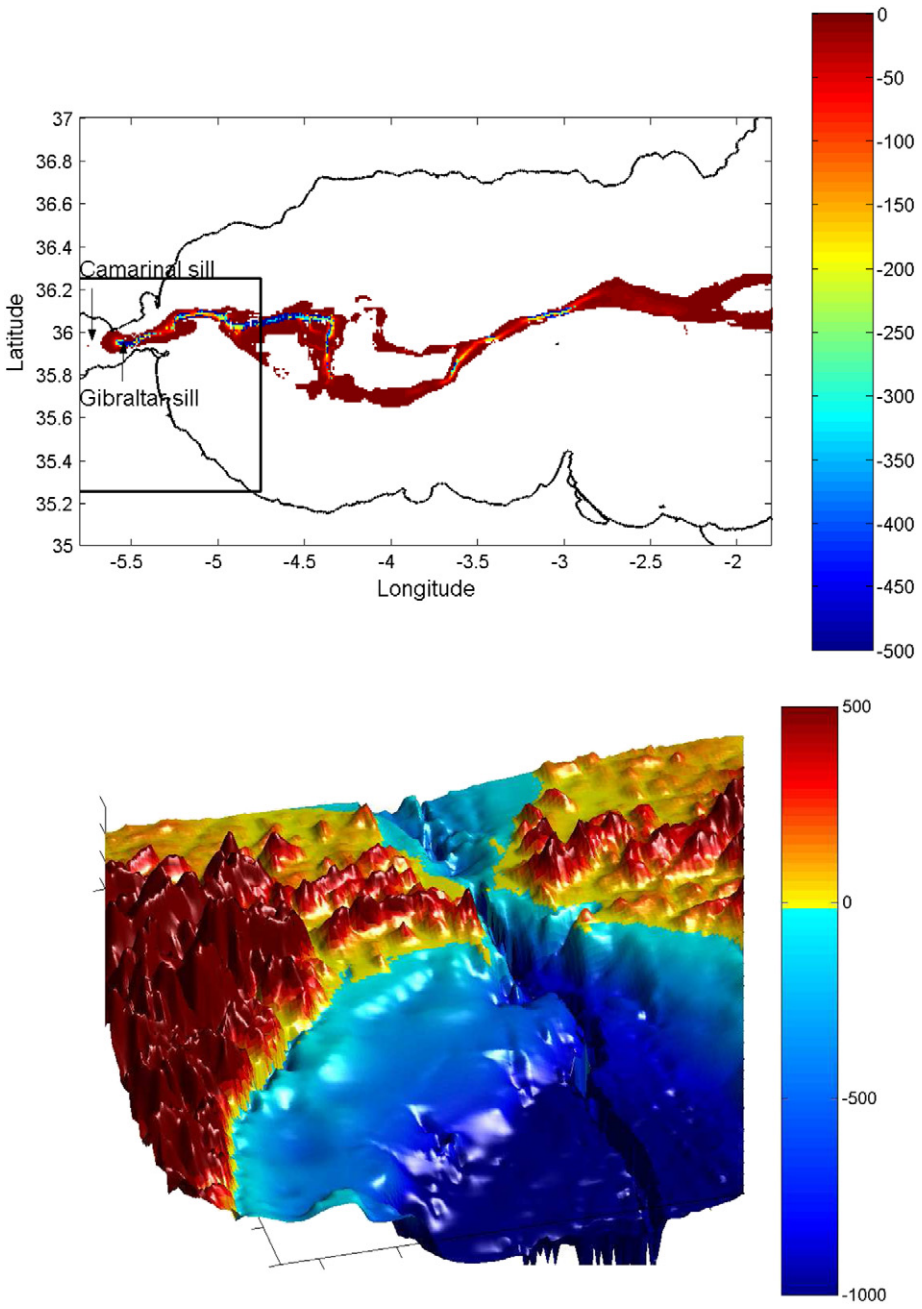

Fig. 8. The computed incised Zanclean Channel (up), and the new topography of the western Alboran Sea (bottom) resulting after 49 years of water inflow reconstructed with the 2D model coupled with the erosion module (Section 3.4). Scale color-bar in m (measured positive above the present sea level in the 3D view, which corresponds to the area defined by the rectangle in the first panel). In the top panel, the color scale gives the topography change in m.

the Zanclean Channel surpass 400 m in most of the transects up to 4.3° W and its width is about 6–8 km. This figure is in reasonable good agreement with data reported by Estrada et al. (2011) taking into account the poor spatial resolution of the 2D model and the simplification of adopting a constant and uniform value for k_b. The incised channel almost vanished between 4.3° W and 3.6° W. This area corresponds to a natural wide topographic low which is flooded since the earliest stages and where water currents are relatively much lower (see Fig. 3). Incision becomes again quite noticeable across the Alboran Ridge. Regressive erosion in Gibraltar is also apparent, although the incised channel is narrower than its current configuration and it does not reach the Camarinal Sill. It can be expected that a more elaborated treatment of lateral erosion should lead to a higher water flow, and to improve results for the erosion along the Zanclean Channel.

3.5. Implications for the open questions on the Zanclean flood of the Mediterranean

Fig. 3 demonstrates the ability of the model for encountering the connected topographical lows which define the path of the Zanclean Channel. This should have been the most likely path followed by the continuous or pulsed inflow of Atlantic waters required to explain the total amount of precipitated salts during the MSC. Although no major riverine systems have been identified, this path also should have concentrated the course of surface waters flowing along the

dessicated Alboran Basin. These flows of water, in the course of tens of ky, should have resulted in an excavated channel (as expected from the work by Loget et al., 2005), over which the Zanclean flood superposed its erosional fingerprint.

Once erosion is initiated, there are not any intrinsic physical stop conditions in the incision model, other than the vanishing of the hydraulic gradient; and the chance of a non-catastrophic stop decreases as the water flow increases. Thus, the transgression of Atlantic waters during the MSC should have been maintained in the range of reversibility, such as with the harmonic coupling between tectonics and erosion in the Gibraltar arc suggested by García-Castellanos and Villaseñor (2011), and/or with the contribution of eustatic sea level changes. The same argument applies for the proposed first step in the reflooding of the Mediterranean, preceding the second catastrophic step, and which should have involved only moderate water flows.

The western transect of the channel, deeply incised across the former isthmus of Gibraltar, can only be explained by a catastrophic Zanclean flood, and a so huge water flow undoubtedly should have resized the preexisting channel. This argument, along with the contribution from other erosional features in the Alboran Basin consuming frictional energy, as the terraces identified by Estrada et al. (2011), allows to use the excavated volume of the Zanclean Channel, V_Z, as a good proxy for constraining, at least in order of magnitude, the value of the ratio f_y/ϵ_v in the coefficient k_b, when the gap of potential gravitational energy, E_P, is provided. Thus, one can expect the ratio f_y/ϵ_v being somewhat lower than V_Z/E_P.

The debate on the sea level fall during the MSC can be better solved by geophysical studies of the Messinian Erosional Surfaces (MES), which provide a value around 1300–1500 m in the western Mediterranean Basin (Estrada et al., 2011; Urgeles et al., 2011). Nevertheless, additional arguments can be provided from the present modelling study. The gap between the Atlantic and the Mediterranean sea levels has to be large enough as to provide the time of opportunity for developing a catastrophic flow of water. The numerical experiment 2D-E4-2 shows that a gap of 1500 m is large enough to produce incision depths over 300 m in the Gibraltar Sill with an energetically-consistent k_b coefficient. On the basis of this numerical experiment, a final incision depth, $z_{s,f}$, of 540 m is achieved with $k_b = 1.4k_{b,0}$, which implies that the ratio $f_y/\epsilon_v = 2.1 \times 10^{-11}$ is ~30% of V_Z/E_P for a gap of 1500 m. The maximum water flow reaches 68.7 Sv and $t_{90} = 15.7$ y. Fig. 9 shows the time evolution of water flow and the sea level at the western and eastern Mediterranean basins for two stated depths at Sicily Sill. This numerical solution will be referred as 2D-E4-3 hereafter.

It is worth noting that the coefficient k_b in the incision law is also contributed by the friction coefficient k_f (Eq. (5)). But this last is independently constrained by the acceptable values for the Manning coefficient (see Appendix B) and by its major effect in the shear stress (see Fig. 5) magnitude, the causal factor in the incision law. The value $k_f = 0.010$ fulfills both requirements well.

The topography of the former isthmus at Gibraltar plays a moderate roll since it affects the required k_b value to produce a final incision of a few hundred meters (see Experiment 2D-E3-2 versus 2D-E4-1 in Table 2). The SS configuration, of a smooth isthmus, is more realistic and it works well with the energy balance, as shown above.

Taking as a reference the numerical experiment 2D-E4-3, sensitivity tests allow characterizing the propagated uncertainties: i) Changes of 10% in k_f imply propagated relative uncertainties of 1.3% if water flow, 10% in shear stress and 16% in the incision rate; ii) changes of 10% in the ratio f_y/ϵ_v do not affect hydrodynamics, but they imply changes of 16% in the final incision depth; iii) changes of 10% in the initial Mediterranean sea level imply propagated relative uncertainties of 12% in the final incision depth.

The attenuation of the water flow after its peak value, due to the vanishing of the hydraulic gradient, is a relatively fast process (about 5 months in experiment 2D-E4-2). Thus, the model does not support any last stage of slow refilling of the Mediterranean at geological scale, as suggested by Cornée et al. (2016).

Concerning the triggering mechanism, the catastrophic flooding conditions leading to an excavated sill of a few hundred meters, are achieved with the initial configuration of a wide sill when the threshold stress is exceeded in the very early stages of the flooding. This requires a water lamina a few meters thick flowing over the sill. These initial conditions cannot be achieved by slow and lasting processes; otherwise the associated inflow increases the Mediterranean

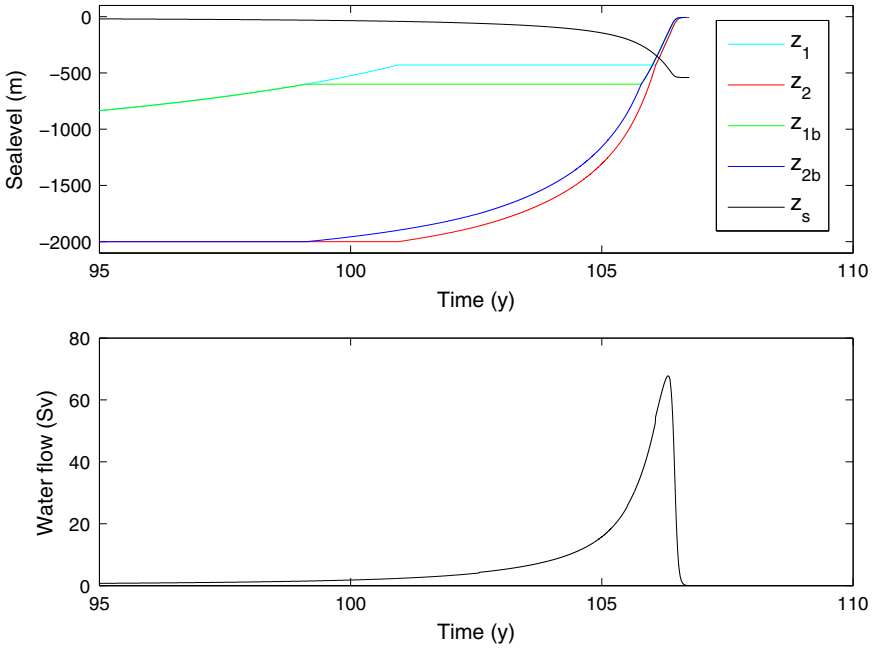

Fig. 9. Temporal evolution of the sea level at the western and eastern Mediterranean basins (z_1 and z_2) for two stated depths at the Sicily Sill (430 m and 600 m — label "b" is added to refer to this last). Time $t = 0$ corresponds to the initial conditions stated for experiment 2D-E4-3. The evolution of the incision depth at the Gibraltar Sill, z_s, and the water flow are also depicted. Both are unaffected by the depth of the Sicily Sill.

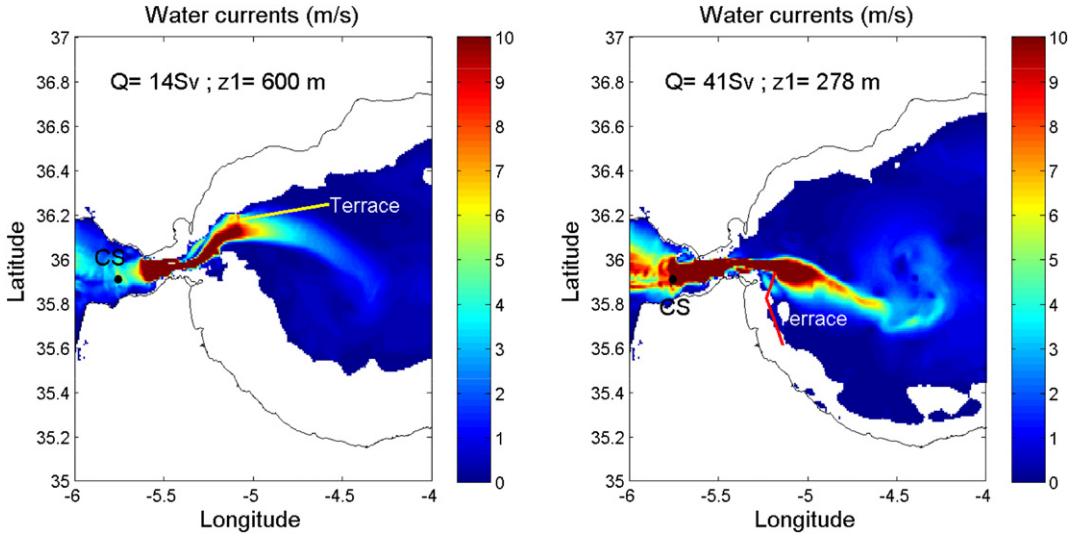

Fig. 10. Computed water current magnitudes (m/s) at the Strait of Gibraltar and the western Alboran Sea at two stages of the Zanclean flood. The water flow and the sea level at the Alboran Sea (meters below the Atlantic Sea level) are depicted in each panel. The terraces identified by Estrada et al. (2011) are shown. The black dot indicates Camarinal Sill (CS) location.

Sea level and reduces the time of opportunity for developing an asymptotic increase in the incision depth. The role of tectonic activity through strike–slip faulting as a triggering process has been already suggested (Balanyá et al., 2007; Luján et al., 2011) . The role of tides in the early stage of the flooding has not been studied here, but a tidal amplitude of up to 1.5 m could be expected in the configuration of an almost closed Strait of Gibraltar. The induced pulsed friction across the sill could have contributed to an enhanced incision rate.

Estrada et al. (2011) identified several submarine terraces in the western Alboran Basin, aligned sub-parallel to the Spanish and Moroccan margins, and likely formed during periods of relative sea level stillstands. Particularly, these authors suggested that the shallower terraces in the Spanish margin (600 m depth) may have formed when the western Mediterranean waters reached the level of the Sicily Sill and started flooding the eastern Mediterranean Basin. While the western Alboran Sea remained desiccated, the inflow of Atlantic waters was confined into the path of the Zanclean Channel, but as the rising sea level flooded the channel, a new 3D pattern of water circulation had to be established. Our present modelling work (Section 3.4) does not explicitly account for the details on the passage of the Sicily Sill, whose paleao-depth remains controversial. But the steady sea level at the western Mediterranean, which arises as a straightforward consequence, cannot justify by itself the formation of terraces, and the 2D structure of the water currents must be also considered. This is illustrated in Fig. 10 where a jet of 14 Sv of Atlantic waters enters to an Alboran Sea with a sea level at 600 m below the Atlantic one. The jet is tangent to the line of terraces. Thus, this hypothesis for the terrace formation seems to be consistent to the extent that such a stillstand sea level can be justified by other geological evidences. But for the shallower terraces in the Moroccan margin (200–300 m depth), there is not a clear justification for a stillstand sea level, and the 2D structure of the Atlantic jet does not seem to be related with the path of the terraces (Fig. 10).

The shape of the Atlantic water jet (Fig. 10) also illustrates how regressive erosion is related with the maximum water flow at Gibraltar Sill. High water currents in this area are observed only for water flows of tens of Sv. Thus, to explain the two incision palaeochannels around the Tartessos Mount, in the Camarinal Sill, as a result of the Zanclean flood, the water flow should have exceeded the value of several tens of Sv. This is consistent with the limitation in the water flow due to the Camarinal Sill, as inferred from Fig. 4, and with the absence of noticeable erosion at this location in the numerical exercise shown in Fig. 8, for which the maximum water flow did not surpassed 15 Sv. The excavation of these palaeochannels also requires enough time of opportunity for the incision process. In the framework of the numerical experiment 2D-E4-3 the cumulated incision is about 100 m, which is lower but of the order of the value reported (250 m) by García-Castellanos et al. (2009).

Although new refinements through a better description of the palaeobathymetry and the spatial variability of erodibility could significantly improve the quality of model outputs, the current modelling experiment 2D-E4-3 is able to produce a reasonable description of the main features of the Zanclean Channel, while it is consistent with the imposed constrains of the initial Mediterranean Sea level and the global energy balance for the incised channel.

4. Conclusions

A new formulation for lateral erosion, involving the shear stress as causal magnitude, has been included in the previously published 0D model for the Zanclean flood (García-Castellanos et al., 2009). Now initial conditions become relevant for the final stage of the flooding. Those consisting of a relatively narrow stream of water crossing the former isthmus at Gibraltar lead to unacceptable final incision depths. Those others representing an initial wide and shallow sill surpassed by a water lamina can lead to a catastrophic flooding scenario.

The 2D-hydrodynamics equations provide a more reliable description of the water flow and the shear stresses for a wide connection channel. A reliable morphology of the former isthmus has to be implemented in the numerical model, which has been achieved through the use of a simple single-parameter algorithm.

Water flow increases with the excavated cross-sectional area at the sill until this last is larger than the section upstream, in the shallow area of Camarinal Sill. The flow attenuation starts to be noticeable when the gap between the Atlantic and the Mediterranean levels is of the order of half the sill depth, and it fits well to an exponential saturation function. This discards any role of the Sicily Sill in the control of the flow at Gibraltar during the Zanclean flood.

The main geological features of the Zanclean Channel, including a sill depth of a few hundred meters at Gibraltar, can be understood

from a scenario of catastrophic flooding of the Mediterranean with the initial conditions of a marine waterway consisting of a wide sill surpassed by a water lamina. An energy balance served for rewriting the incision law and to constrain the values of the involved parameters. The initial water level at the Mediterranean must be low enough to allow a time of opportunity for developing an asymptotic increase in the incision depth. The value of a sea level fall of 1300–1500 m at the western Mediterranean, supported by MES studies, fits well the model requirements. The threshold stress to initialize erosion must be exceeded in the very early stages of the flooding. This implies a water lamina a few meter thick. These initial conditions hardly can be achieved by slow and lasting processes since the associated inflow can significantly increase the Mediterranean Sea level. Tectonics may have play a major role through strike-slip faulting, as suggested by other authors.

Appendix A. 0D model

The mathematical model published by García-Castellanos et al. (2009) and revisited by Periáñez and Abril (2015) is summarized here. It considers a sill of width W and average depth z_s, connecting the Atlantic and the Mediterranean basins. The last is divided into two water bodies, separated by the Sicily Sill, with respective free water levels at z_1 and z_2 (with all z_i, $i = 0, 1, 2, s$ measured positive below the mean sea level at the Atlantic Ocean, z_0). The mean water current over the sill, v_s, is estimated from the Manning's formula:

$$v_s = \frac{1}{n} R_h^{2/3} S^{1/2}, \tag{8}$$

where $n = 0.05$ is the roughness coefficient, and $R_h \simeq z_s - z_0$ is the hydraulic radius. S is the hydraulic gradient, estimated as $S = (z_1 - z_0)/L$, with $L = 100$ km, which maximizes the half-width of the Betic-Rifean orogen. When $z_1 - z_0 > 1000$ m, S is set as 0.01. The shear stress at the sill, τ_b, is

$$\tau_b = \rho g (z_s - z_0) S, \tag{9}$$

where ρ is the density of water, and g the acceleration of gravity. This stress induces erosion on the sill seabed at a rate:

$$\frac{dz_s}{dt} = k_b (\tau_b)^a, \tag{10}$$

with $a = 1.5$ and $k_b = 1.30 \times 10^{-4}$ m y^{-1} Pa^{-a} in the reference model. The water flow, Q, can be then estimated as $Q = W(z_s - z_0)v_s$. The width of the sill irreversibly increases as $W = k_w Q^{a_w}$, with $k_w = 1.2$ and $a_w = 0.5$.

Initial values $z_0 = 0$, $z_1 = 2500$ m and $z_2 = 2700$ m are adopted as being representative of the situation at the end of the Messinian salinity crisis (García-Castellanos et al., 2009). The initial values of z_s and W have to be provided. The incoming water flow, Q, results in the filling of the Mediterranean basin following the hypsometric curves given by Meijer and Krijgsman (2005) with a stated depth for the Sicily Sill of $z_{sc} = 430$ m.

Corrections due to the Bernoulli effect and the head loss by friction have been introduced as in Periáñez and Abril (2015). Both contribute to a decrease in the free water level at the sill. Thus it is necessary to distinguish between excavated and wet cross-sections and consistently update the estimations for Q and τ_b.

By inserting Eq. (9) into Eq. (10), one can solve for z_s under constant S:

$$\frac{1}{z_s^{a-1}} = \frac{1}{z_{s,0}^{a-1}} - \beta t; \beta = (a-1) k_b (\rho g S)^a, \tag{11}$$

where $z_{s,0}$ is the value of z_s for $t = 0$. This solution has a vertical asymptote for $t_L = 1 / (\beta z_{s,0}^{a-1})$. For $z_{s,0} = 1.0$, $a = 3/2$ and $S = 0.01$, $t_L = 15.2$ y. The decrease of S as filling proceeds prevents reaching infinity values for z_s.

Writing Q in terms of W and z_s using Eq. (8) and inserting the scaling law for the channel width, the following relationship arises:

$$\frac{dW}{dt} = \frac{5 a_w}{3 - 3 a_w} \frac{W}{z_s} \frac{dz_s}{dt}. \tag{12}$$

With $a_w = 0.5$ and the aspect ratio for the Gibraltar Strait $W/z_s \sim 50$, the lateral erosion is almost two orders of magnitude higher than the vertical incision.

Appendix B. 2D model

Computational fluid dynamic models which simulate catastrophic flood events have been applied to dam-breaking with high spatial and temporal resolutions (for instance Biscarini et al., 2010). For larger spatial and temporal scales, as those involved in the Zanclean flood of the Mediterranean, a two-dimensional depth-averaged hydrodynamic model represents a suitable approach, as shown by Periáñez and Abril (2015). The selected model is an adaptation from a previous one devoted to tsunami propagation, and it has resulted to be a very robust computational tool (Periáñez and Abril, 2013, 2014a,b) .

The two components of the depth-averaged water current(u, v, in the east–west and south–north directions, respectively), along with the water surface elevation above the reference level, ζ, are given by the equations for conservation of mass and momentum:

$$\frac{\partial \zeta}{\partial t} + \frac{\partial}{\partial x}(Du) + \frac{\partial}{\partial y}(Dv) = 0 \tag{13}$$

$$\frac{\partial u}{\partial t} + u\frac{\partial u}{\partial x} + v\frac{\partial u}{\partial y} + g\frac{\partial \zeta}{\partial x} - \Omega v + \frac{\tau_u}{\rho D} = A\left(\frac{\partial^2 u}{\partial x^2} + \frac{\partial^2 u}{\partial y^2}\right) \tag{14}$$

$$\frac{\partial v}{\partial t} + u\frac{\partial v}{\partial x} + v\frac{\partial v}{\partial y} + g\frac{\partial \zeta}{\partial y} + \Omega u + \frac{\tau_v}{\rho D} = A\left(\frac{\partial^2 v}{\partial x^2} + \frac{\partial^2 v}{\partial y^2}\right), \tag{15}$$

where h is the undisturbed water depth, ζ is the displacement of the water surface above the undisturbed sea level measured upwards, $D = h + \zeta$ is the total water depth, Ω is the Coriolis parameter ($\Omega = 2w\sin\lambda$, where w is the Earth rotational angular velocity and λ is latitude) and A is the horizontal eddy viscosity. τ_u and τ_v are friction stresses which have been written in terms of a quadratic law:

$$\tau_u = k_f \rho u \sqrt{u^2 + v^2}$$
$$\tau_v = k_f \rho v \sqrt{u^2 + v^2} \tag{16}$$

where k_f is the bed friction coefficient. All the equations are solved numerically using explicit finite difference schemes (Kowalik and Murty, 1993) with second order accuracy. In particular, the MSOU (Monotonic Second Order Upstream) is used for the advective non-linear terms in the momentum equations. A wetting/drying algorithm is implemented following the numerical scheme described in Kampf (2009).

Values of $k_f = 0.0025$ and $A = 10$ m^2/s have widely proved their use in models for tide and tsunami propagation (e.g. Periáñez and Abril, 2013, 2014a,b) These have been adopted as reference values in this work. Wan and Liu (2014) applied the inverse problem technique in a tidal model to investigate the effect of bottom friction coefficient in the Bohai, Yellow, and East China Seas. They found a spatial distribution with values ranging from 0.0002 up to 0.0018.

For the same region, Zhang et al. (2011) had reported values ranging from 0.001 up to 0.005.

Although they represent different modelling approaches, the friction coefficient in the 2D model, k_f, can be related to the Manning coefficient, n, as $k_f = gn^2/D^{1/3}$ (Mayo et al., 2014). The recommended value of n for bare rocks and sand is 0.04 (with a range from 0.03 to 0.07). García-Castellanos et al. (2009) used $n = 0.05$ as being representative for mountain bedrock rivers. For a water lamina over few tens meters, changes of k_f with D are small, which justifies the approach of adopting a constant depth-independent value, as it is quite usual in 2D hydrodynamic models for marine environments. The reference value of $k_f = 0.0025$ approximately corresponds to $n = 0.03 - 0.04$ with D over 40 m, while $k_f = 0.01$ can reproduce a range of scenarios such as $n = 0.05$ with $D \sim 10$ m or $n = 0.07$ with $D \sim 100$ m. Thus, within the adopted simplification of using a constant and uniform value for k_f, the two selected scenarios ($k_f = 0.0025$ and $k_f = 0.01$) fit well to the reported range of values for the Manning coefficient in bedrock waterways.

Boundary conditions along the Strait of Gibraltar (western open boundary, at 6° W) are imposed by fixing the Atlantic Ocean level. The Mediterranean Sea level is also prescribed along the open boundary in the eastern side of the domain, but it is allowed to change with the Atlantic inflow following the hypsometric curves given by Meijer and Krijgsman (2005), as shown in Periáñez and Abril (2015).

References

Annandale, G., 1995. Erodibility. J. Hydraul. Res. 33 (4), 471–494.

Cak.r, Z., Bache, F., Popescu, S.M., Rabineau, M., Gorini, C., Suc, J.P., Clauzon, G., Olivet, J.-L., Rubino, J.-L., Melinte-Dobrinescu, M.C., Estrada, F., Londeix, L., Armijo, R., Meyer, B., Jolivet, L., Jouannic, G., Leroux, E., Aslanian, D., Reis, A.T.D., Mocochain, L., Zagorchev, I., Brun, J.-P., Sokoutis, D., Csato, I.T., Ucarkus, G., 2012. A two-step process for the reflooding of the Mediterranean after the Messinian Salinity Crisis. Basin Res. 24, 125–153.

Balanyá, J.C., Crespo-Blanc, A., Díaz-Azpiroz, M., Expósito, I., Luján, M., 2007. Structural trend line pattern and strain partitioning around the Gibraltar Arc accretionary wedge: insights as to the mode of orogenic arc building. Tectonics 26, 1–19.

Biscarini, C., Di Francesco, S., Manciola, P., 2010. CFD modelling approach for dam break flow studies. Hydrol. Earth Syst. Sci. 14, 705–718.

Blanc, P.L., 2002. The opening of the Plio-Quaternary Gibraltar Strait: assessing the size of a cataclysm. Geodin. Acta 15, 303–317.

Blanc, P.L., 2006. Improved modelling of the Messinian Salinity Crisis and conceptual implications. Palaeogeogr. Palaeoclimatol. Palaeoecol. 238, 349–372.

Carnevale, G., Landini, W., Sarti, G., 2006. Mare versus Lago-Mare: marine fishes and the Mediterranean environment at the end of the Messinian Salinity Crisis. J. Geol. Soc. Lond. 163, 75–80.

Carnevale, G., Longinelli, A., Caputo, D., Barbieri, M., Landini, W., 2008. Did the Mediterranean marine reflooding precede the Mio-Pliocene boundary? Paleontological and geochemical evidence from upper Messinian sequences of Tuscany, Italy. Palaeogeogr. Palaeoclimatol. Palaeoecol. 257, 81–105.

Cornée, J.J., Münch, Ph, Achalhi, M., Merzeraud, G., Azdimousa, A., Quillévéré, F., Melinte-Dobrinescu, M., Christian Chaix, Ch, BenMoussa, A., Lofi, J., Séranne, M., Moissette, P., 2016. The Messinian erosional surface and early Pliocene reflooding in the Alboran Sea: new insights from the Boudinar basin. Morocco. Sedimentary Geology 333, 115–129.

Crespo-Blanc, A., Campos, J., 2001. Structure and kinematics of the South Iberian paleomargin and its relationship with the Flysch Trough units: extensional tectonics within the Gibraltar Arc fold-and-thrust belt (western Betics). J. Struct. Geol. 23, 1615–1630.

Esteras, M., Izquierdo, J., Sandoval, N.G., Bahmad, A., 2000. Evolución morfológica y estratigráfica pliocuaternaria del umbral de camarinal (estrecho de Gibraltar) basada en sondeos. Marinos. Rev. Soc. Geol. España 13, 539–550.

Estrada, F., Ercilla, G., Gorini, C. h. r., Alonso, B., Vázquez, J.T., García-Castellanos, D., Juan, C., Maldonado, A., Ammar, A., Elabbassi, M., 2011. Impact of pulsed Atlantic water inflow into the Alboran Basin at the time of the Zanclean flooding. Geo-Mar. Lett. 31, 361–376.

Finnegan, N.J., Dietrich, W. e., 2011. Episodic bedrock strath terrace formation due to meander migration and cutoff. Geology 39, 143–146.

Finnegan, N.J., Roe, G., Montgomery, D.R., Hallet, B., 2005. Controls on the channel width of rivers: implications for modeling fluvial incision bedrock. Geology 33, 229–232.

García-Castellanos, D., Estrada, F., Jiménez-Munt, I., Gorini, C., Fernández, M., Vergés, J., De vicente, R., 2009. Catastrophic flood of the Mediterranean after the Messinian Salinity Crisis. Nature 462. http://dx.doi.org/10.138/nature08555.

García-Castellanos, D., Villaseñor, A., 2011. Messinian Salinity Crisis regulated by competing tectonics and erosion at the Gibraltar Arc. Nature Letters 480, 359–363.

Guerra-Merchán, A., Serrano, F., Hlila, L., El Kadiri, K., Sanz de Galdeano, C., Garcés, M., 2014. Tectono-sedimentary evolution of the peripheral basins of the Alboran Sea in the Arc of Gibraltar during the latest Messinian–Pliocene. J. Geodyn. 77, 158–170.

Kampf, J., 2009. Ocean Modelling for Beginners. Springer-Verlag, Heidelberg.

Konsoer, K.M., Rhoads, b. L., Langendoen, E.J., Best, J.L., Urisc, M.E., Abad, J.D., Garcia, M.H., 2016. Spatial variability in bank resistance to erosion on a large meandering mixed bedrock–alluvial river. Geomorphology 252, 80–97.

Kowalik, Z., Murty, T.S., 1993. Numerical Modelling of Ocean Dynamics. World Scientific, Singapore.

Lague, D., 2013. The stream power river incision model: evidence, theory and beyond. Earth Surf. Process. Landf. 39, 38–61.

Lamb, M.P., Dietrich, W.E., Sklar, L.S., 2008. A model for fluvial bedrock incision by impacting suspended and bed load sediment. J. Geophys. Res. 113, F03025. http://dx.doi.org/10.1029/2007JF000915.

Lamb, M.P., Finnegan, N.J., Scheingross, J.S., Sklar, L.S., 2015. New insights into the mechanics of fluvial bedrock erosion through flume experiments. Geomorphology 244, 33–55.

Lavé, J.P., Avouac, J.P., 2001. Fluvial incision and tectonic uplift across the Himalayas of central Nepal. J. Geophys. Res. 106, 26561–26591.

Liao, Ch.T., Yeh, K.C.h., Huang, M.W., 2014. Development and application of 2-D mobile-bed model with bedrock river evolution mechanism. J. Hydro Environ. Res. 8, 210–222.

Loget, N., Den Driessche, J.V., 2006. On the origin of the Strait of Gibraltar. Sediment. Geol. 188-189, 341–356.

Loget, N., Den Driessche, J.V., Davi, P., 2005. How did the salinity crisis end? Terra Nova 17, 414–419.

Luján, M., Crespo-Blanc, A., Comas, M., 2011. Morphology and structure of the Camarinal Sill from high-resolution bathymetry: evidence of fault zones in the Gibraltar Strait. Geo-Mar. Lett. 31, 163–174.

Manzi, V., Lugli, S., Ricci Lucchi, F., Roveri, M., 2005. Deep-water clastic evaporates deposition in the Messinian Adriatic foredeep (northern Apennines, Italy): did the Mediterranean ever dry out? Sedimentology 52, 875–902.

Mayo, T., Butler, T., Dawson, C., Hoteit, I., 2014. Data assimilation within the Advanced Circulation (ADCIRC) modeling framework for the estimation of Manning's friction coefficient. Ocean Model. 76, 43–58.

Meijer, P.T., Krijgsman, W., 2005. A quantitative analysis of the desiccation and re-filling of the Mediterranean during the Messinian Salinity Crisis. Earth Planet. Sci. Lett. 240, 510–520.

Pérez-Asensio, J.N., Aguirre, J., Jiménez-Moreno, G., Schmiedl, G., Civis, J., 2013. Glacioeustatic control on the origin and cessation of the Messinian Salinity Crisis. Global Planet. Change 111, 1–8.

Periáñez, R., Abril, J.M., 2013. Modelling tsunami propagation in the Iberia–Africa plate boundary: historical events, regional exposure and the case-study of the former Gulf of Tartessos. J. Mar. Syst. 111-112, 223–234.

Periáñez, R., Abril, J.M., 2014a. Modelling tsunamis in the Eastern Mediterranean Sea. Application to the Minoan Santorini tsunami sequence as a potential scenario for the biblical Exodus. J. Mar. Syst. 139, 91–102.

Periáñez, R., Abril, J.M., 2014b. A numerical modelling study on oceanographic conditions in the former Gulf of Tartessos (SW Iberia): tides and tsunami propagation. J. Mar. Syst. 139, 68–78.

Periáñez, R., Abril, J.M., 2015. Computational fluid dynamics simulations of the Zanclean catastrophic flood of the Mediterranean (5.33 Ma). Palaeogeogr. Palaeoclimatol. Palaeoecol. 424, 49–60.

Roveri, M., Flecker, R., Krijgsman, W., Lofi, J., Lugli, S., Manzi, V., Sierro, F.J., Bertini, A., Camerlenghi, A., De Lange, G., Govers, R., Hilgen, F.J., Hübscher, Chr, Meijer, P.T.h., Stoica, M., 2014. The Messinian Salinity Crisis: past and future of a great challenge for marine sciences. Mar. Geol. 352, 25–58.

Urgeles, R., Camerlenghi, A., García-Castellanos, D., De Mol, B., Garcés, M., Vergés, J., Haslam, I., Hardman, M., 2011. New constraints on the Messinian sealevel drawdown from 3d seismic data of the Ebro Margin, western Mediterranean. Basin Res. 23, 123–145.

Lü, Wan, D., Liu, Q., 2014. A study on bottom friction coefficient in the Bohai, Yellow, and East China Seas. Math. Probl. Eng. 7.432529. http://dx.doi.org/10.1155/2014/432529.

Whittaker, A.C., Cowie, P.A., Attal, M., Tucker, G.E., Roberts, G.P., 2007. Bedrock channel adjustment to tectonic forcing: implications for predicting river incision rates. Geology 35, 103–106.

Wobus, C.W., Tucker, G.E., Anderson, R.S., 2006. Self-formed bedrock channels. Geophys. Res. Lett. 33, 6.L18408.

Zhang, J., Lu, X., Wang, Y.P., 2011. Study on linear and non linear bottom friction parameterizations for regional tidal models using data assimilation. Cont. Shelf Res. 31, 555–573.